MOLECULAR AND CELLULAR BIOLOGY, Mar. 1997, p. 1354–1365 Vol. 17, No. 3
0270-7306/97/$04.00+0

Dbp3p, a Putative RNA Helicase in *Saccharomyces cerevisiae*, Is Required for Efficient Pre-rRNA Processing Predominantly at Site A_3

PAUL L. WEAVER,[1] CHAO SUN,[2]† AND TIEN-HSIEN CHANG[1]*

Department of Molecular Genetics, The Ohio State University, Columbus, Ohio 43210,[1] and Department of Biological Sciences, Mellon Institute, Carnegie Mellon University, Pittsburgh, Pennsylvania 15213[2]

Received 25 September 1996/Returned for modification 1 November 1996/Accepted 3 December 1996

In *Saccharomyces cerevisiae*, ribosomal biogenesis takes place primarily in the nucleolus, in which a single 35S precursor rRNA (pre-rRNA) is first transcribed and sequentially processed into 25S, 5.8S, and 18S mature rRNAs, leading to the formation of the 40S and 60S ribosomal subunits. Although many components involved in this process have been identified, our understanding of this important cellular process remains limited. Here we report that one of the evolutionarily conserved DEAD-box protein genes in yeast, *DBP3*, is required for optimal ribosomal biogenesis. *DBP3* encodes a putative RNA helicase, Dbp3p, of 523 amino acids in length, which bears a highly charged amino terminus consisting of 10 tandem lysine-lysine-X repeats ([KKX] repeats). Disruption of *DBP3* is not lethal but yields a slow-growth phenotype. This genetic depletion of Dbp3p results in a deficiency of 60S ribosomal subunits and a delayed synthesis of the mature 25S rRNA, which is caused by a prominent kinetic delay in pre-rRNA processing at site A_3 and to a lesser extent at sites A_2 and A_0. These data suggest that Dbp3p may directly or indirectly facilitate RNase MRP cleavage at site A_3. The direct involvement of Dbp3p in ribosomal biogenesis is supported by the finding that Dbp3p is localized predominantly in the nucleolus. In addition, we show that the [KKX] repeats are dispensable for Dbp3p's function in ribosomal biogenesis but are required for its proper localization. The [KKX] repeats thus represent a novel signaling motif for nuclear localization and/or retention.

In eukaryotes, ribosomal biogenesis takes place primarily in a specialized subnuclear compartment termed the nucleolus, where rRNA genes are localized and first transcribed into a single precursor rRNA (pre-rRNA). In *Saccharomyces cerevisiae*, this pre-rRNA is rapidly associated with a large number of ribosomal and nonribosomal proteins and sequentially processed through a number of intermediates by both exo- and endonucleases into mature 25S, 18S, and 5.8S rRNAs which are found in 60S (25S and 5.8S rRNAs) and 40S (18S rRNA) ribosomal subunits (reviewed in reference 79). During transcription and processing, pre-rRNA is also chemically modified by methylation on base and ribose moieties and by pseudouridylation. Although this highly complicated rRNA-processing pathway has been studied with many organisms, the genetically tractable yeast system has so far provided the most extensive information regarding the various *cis*- and *trans*-acting factors crucial to this process.

In yeast, rRNA is first transcribed by RNA polymerase I as a 35S pre-rRNA which contains the mature 18S, 5.8S, and 25S rRNAs separated by two internal transcribed spacers, ITS1 and ITS2, and flanked by two external transcribed spacers, 5′ ETS and 3′ ETS (Fig. 1) (reviewed in reference 74). Processing of this 35S pre-rRNA occurs initially at sites A_0, A_1, and A_2 to yield the 20S pre-rRNA and the $27SA_2$ pre-rRNA. Processing of the 20S pre-rRNA takes place in the cytoplasm, where site D is cleaved to form the mature 18S rRNA, whereas the $27SA_2$ pre-rRNA continues to be processed in the nucleolus by two alternative pathways. The major pathway involves cleavage at sites A_3 and B_2, yielding the $27SA_3$ precursor, which is rapidly converted to $27SB_S$ pre-rRNA by exonuclease activities. The minor pathway involves cleavage at sites $B1_L$ and B_2 to produce the $27SB_L$ pre-rRNA. Both $27SB_S$ and $27SB_L$ pre-rRNAs are further cleaved at sites C_1 and C_2 to release the mature 25S rRNA and $7S_S$ or $7S_L$ species, which is then processed by an exonuclease to site E, yielding the mature $5.8S_S$ or $5.8S_L$ rRNA.

A large number of *trans*-acting factors have been shown to be involved in the yeast pre-rRNA-processing pathway (reviewed in references 15 and 74). Many of these are small nucleolar RNAs (snoRNAs), which are associated with proteins to form ribonucleoprotein particles (snoRNPs). It has been shown that genetic depletions of four snoRNAs, i.e., U3 (5, 26), U14 (38), snR10 (68), and snR30 (46), and their associated proteins, i.e., Nop1p (59), Gar1p (20), and Sof1p (29), inhibit or delay cleavages at sites A_0, A_1, and A_2, which in turn results in the reduction of 18S rRNA without a major impact on 25S and 5.8S rRNA synthesis. Interestingly, cleavage at site A_3 is mediated by another snoRNP, the RNase MRP, as mutations occurring in its RNA (13, 40, 61, 63) or protein (41, 62) components inhibit the cleavage, resulting in a deficiency of the major $5.8S_S$ species. Recently, this cleavage event has been reproduced in vitro by using purified RNase MRP, convincingly demonstrating a direct role for RNase MRP at the A_3-site cleavage (42). Although apparently mediated by different factors, cleavages at sites A_2 and A_3 appear to be linked, since substitution mutations at either site can inhibit cleavage at the other site (1, 2). These data suggest that efficient cleavage of both A_2 and A_3 sites requires the interaction between a snoRNP complex, bound at sites including A_2, and an RNase MRP complex, bound at site A_3 (2).

In addition to these snoRNP components, there exist a

* Corresponding author. Mailing address: Department of Molecular Genetics, The Ohio State University, 484 West 12th Ave., Columbus, OH 43210. Phone: (614) 292-0631. Fax: (614) 292-4466. E-mail: chang.108@osu.edu.

† Present address: Whitehead Biomedical Institute, Cambridge, MA 02142.

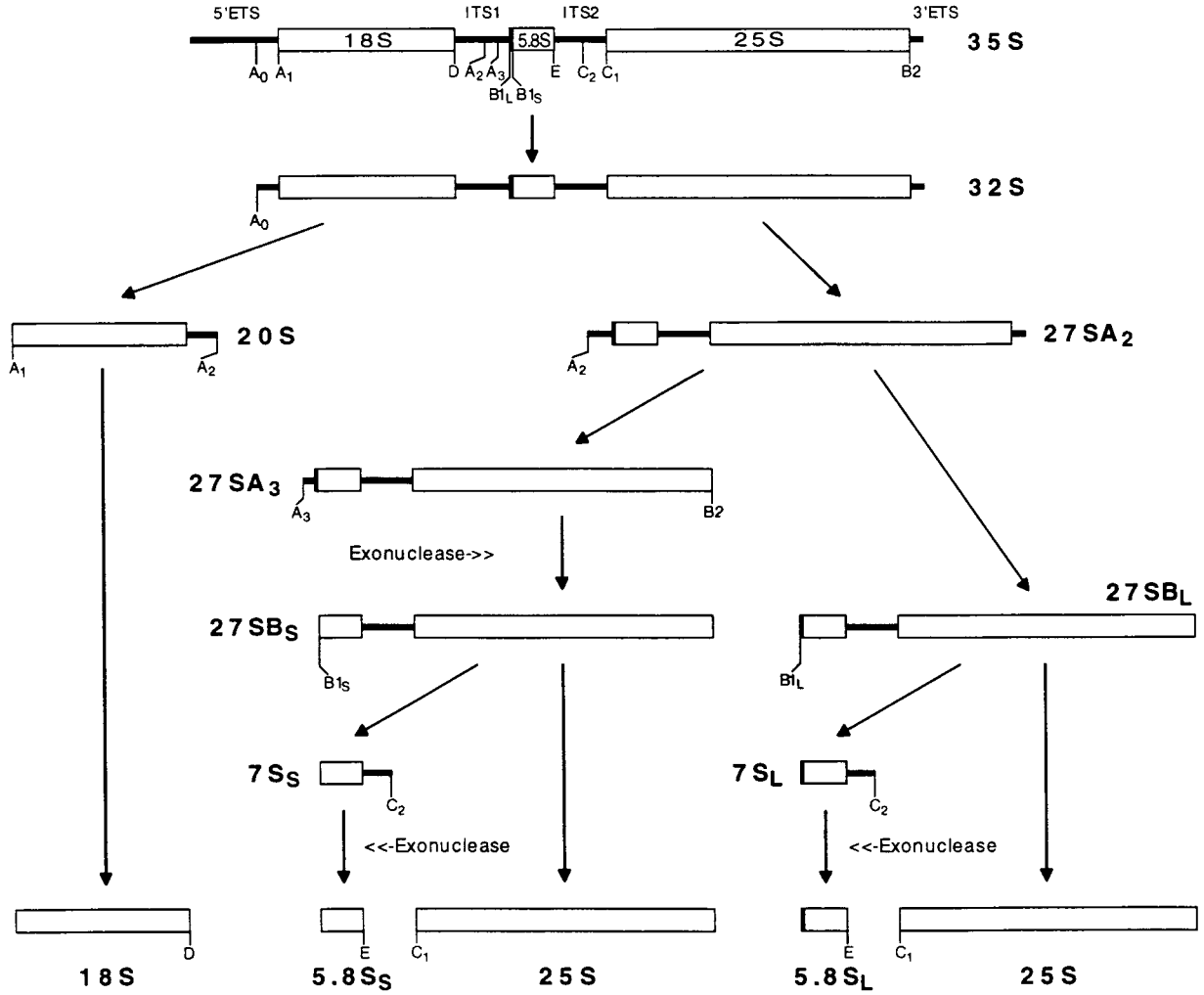

FIG. 1. Pre-rRNA-processing pathway in *S. cerevisiae*. The pre-rRNA transcript is synthesized initially as a 35S precursor containing 18S, 5.8S, and 25S rRNAs flanked by 5′ ETS and 3′ ETS and interrupted by ITS1 and ITS2. Empty bars represent the mature rRNA sequences, and thick lines represent the transcribed spacers. Cleavage sites on the pre-rRNAs and steps which are mediated by exonucleases are indicated. See the text for a detailed description of the pathway.

growing number of snoRNAs predicted to have important roles in rRNA folding, rRNA processing, and ribosomal RNP assembly (4). While some of these snoRNAs have been shown to be responsible for the 2′-O methylation on specific residues of the rRNA (33), others have been proposed to act as RNA chaperones to catalyze the apparent major rearrangements of rRNA at various stages of ribosome synthesis. Enzymes that are predicted to unwind RNA-RNA base pairing, such as the RNA helicases, are likely to play a major role in this process as well. In this regard, a new class of proteins, the DEAD-box proteins (DBPs), may fulfill such a role in ribosomal biogenesis.

Members of the growing *DBP* gene family have considerable sequence similarity and have been found in organisms ranging from *Escherichia coli* to humans (17). Several of these DBPs, such as the mammalian and yeast eIF-4A (7, 53), human p68 (24), *Xenopus* An3 (21), and *Drosophila* vasa (39), have been shown to exhibit RNA-unwinding activities in vitro. Thus, it is generally believed that members of this DBP family are all RNA helicases, whose functions are to modulate specific RNA secondary structures in their respective biochemical pathways, which include translation initiation, nuclear pre-mRNA splicing, and ribosomal biogenesis (17). Multiple DBPs have also been implicated in *E. coli* ribosomal biogenesis. For example, SrmB can suppress a 50S ribosomal subunit assembly mutant (49), and DeaD was isolated as a dosage-dependent suppressor of a ribosomal protein S2 mutant (71). Interestingly, the ATPase activity of the *E. coli* DbpA can be activated only by 23S rRNA, suggesting that it also plays a role in some ribosomal events (18). Likewise, at least two DBPs are required for ribosomal biogenesis in yeast. It has been shown that mutations in *SPB4*, which was isolated as a suppressor of a poly(A)-binding protein mutant (55), and in *DRS1*, which was identified in a screen for cold-sensitive mutants deficient in ribosome subunits (51), significantly decrease the level of 60S ribosomal subunits and inhibit 25S rRNA production.

To date, more than 20 *DBP* genes have been discovered in yeast, and nearly all of them are essential for yeast's survival (11, 17, 60). We report here that deletion of the *DBP3* gene has a major impact on the 60S ribosomal subunit biogenesis resulting from a delay in the production of 25S rRNA. This delay is apparently due to inefficient cleavage at site A_3 and, to a lesser degree, at site A_2, two sites which have been shown to be genetically linked during pre-rRNA processing (2). Further-

more, we show that the predominant nucleolar localization of Dbp3p is mediated at least in part by a novel signaling motif, the lysine-lysine-X repeats ([KKX] repeats).

MATERIALS AND METHODS

Construction of the *dbp3::HIS3* allele and gene replacement. The full-length wild-type *DBP3* gene carried on a 3.72-kb *Bam*HI fragment was obtained from M. Johnston (Washington University, St. Louis, Mo.) and subcloned into the pBluescript KS(+) vector (Stratagene, La Jolla, Calif.) to yield pCA3001. To construct the *dbp3::HIS3* allele, we first subcloned a 2.1-kb *Sal*I-*Xba*I fragment containing the entire *DBP3* gene into the pBluescript KS(+) vector to yield pCA3002. From pCA3002, we removed an internal 1.2-kb *Pst*I-*Hpa*I fragment of *DBP3* and replaced it with a 1.7-kb *Bam*HI fragment containing a functional *HIS3* gene to yield pCA3004. To replace *DBP3* by homologous recombination, the 2.6-kb *Sal*I-*Xba*I fragment containing the *dbp3::HIS3* allele from pCA3004 was used to transform a wild-type diploid strain, YPH274 (*MAT***a**/α *ura3-52/ura3-52 lys2-801/lys2-801 ade2-101/ade2-101 trp1-Δ1/trp1-Δ1 his3-Δ200/his3-Δ200 leu2-Δ1/leu2-Δ1*) (64). The His^+ transformants were screened for the correct replacement of one of the two *DBP3* genes by Southern analysis with a ^{32}P-labeled 2.1-kb *Sal*I-*Xba*I fragment from pCA3002 as a probe. The heterozygous strain, YTC68, containing the *dbp3::HIS3* allele, bears the following genotype: *MAT***a**/α *dbp3::HIS3/DBP3 ura3-52/ura3-52 lys2-801/lys2-801 ade2-101/ade2-101 trp1-Δ1/trp1-Δ1 his3-Δ200/his3-Δ200 leu2-Δ1/leu2-Δ1*.

Tetrad and Northern analyses. Strain YTC68 was sporulated in 1% liquid potassium acetate at 30°C for 2 days. The resulting tetrads were dissected on YPD (1% yeast extract, 2% Bacto Peptone, 2% glucose) plates which were then incubated at either 30, 25, or 15°C until colonies formed on the plates. Genotypes of the segregants were identified by replica plating with various nutrient-dropout synthetic medium plates. Segregants bearing the *dbp3::HIS3* disruption allele, YTC201 (*MAT***a** *dbp3::HIS3 ura3-52 lys2-801 ade2-101 trp1-Δ1 his3-Δ200 leu2-Δ1*) and YTC202 (*MAT*α *dbp3::HIS3 ura3-52 lys2-801 ade2-101 trp1-Δ1 his3-Δ200 leu2-Δ1*), were used in subsequent experiments. To examine for the presence of the *DBP3* transcript, four segregants isolated from a dissected tetrad were grown individually in 2 ml of YPD liquid medium at 30°C to an optical density at 600 nm (OD_{600}) of ~0.75. Total RNAs were isolated by hot phenol-chloroform extraction as described previously (77). Equal amounts of total RNA were denatured with glyoxal, separated by agarose gel electrophoresis, and transferred to a nylon membrane as described previously (56). RNAs were cross-linked to the membrane by UV irradiation and hybridized with a [α-^{32}P]dCTP-labeled probe (the *Bam*HI fragment from pCA3001) synthesized by using a random-priming labeling kit (United States Biochemicals). Hybridization was done overnight at 65°C in 0.1 M sodium phosphate (pH 7.0)–0.5 M NaCl–6 mM EDTA–1% sodium dodecyl sulfate (SDS). The membrane was washed once in 0.25 M sodium phosphate (pH 7.0)–0.125 M NaCl–1.5 mM EDTA–0.25% SDS for 1 h and twice (1 h each) in the same solution without SDS at 65°C.

The oligonucleotides used for analyzing mature and pre-rRNAs were as follows: 18S-A and 25S-A correspond to oligonucleotides a and g, respectively, as described by Bergès et al. (6); ETS1-A corresponds to oligonucleotide a as described by Lafontaine et al. (35); ITS1-A and ITS1-B correspond to oligonucleotides b and c, respectively, as described by Allmang et al. (1); and ITS1-C and 5.8S-A correspond to oligonucleotides 011 and 017, respectively, as described by Lindahl et al. (40). Hybridization and washes were carried out as described by Chang et al. (10) except at room temperature.

Primer extension analysis. Typically, 10 pmol of ^{32}P-labeled oligonucleotides complementary to various regions of pre-rRNAs were annealed to 4 μg of total RNA in a 12-μl reaction mixture containing 0.3 M NaCl, 10 mM Tris-HCl (pH 7.5), and 2 mM EDTA. Primer extensions were initiated by the addition of a reaction mix (40 μl) containing 12.5 mM dithiothreitol, 7.5 mM $MgCl_2$, 12.5 mM Tris-HCl (pH 8.4), 1.25 mM deoxynucleoside triphosphates, 100 U of reverse transcriptase (SuperScript II; Bethesda Research Laboratories), and 20 U of RNasin (Promega). The reaction mixtures were then incubated at 46°C for 40 min. Primer extension products were analyzed on a sequencing gel.

Sucrose gradient analysis. Yeast cultures were grown in 200 ml of YPD or an appropriate synthetic medium to an OD_{600} of ~0.75. One milliliter of 10-mg/ml cycloheximide was added to the culture just prior to harvesting of the cells. The harvested cells were washed twice with buffer II (10 mM Tris-HCl [pH 7.5], 100 mM NaCl, 30 mM $MgCl_2$, 50 μg of cycloheximide per ml, 200 μg of heparin per ml, and 0.2% diethylpyrocarbonate). The washed cells were resuspended in 1.5 ml of buffer II, and an equal volume of glass beads (Sigma; 425 to 600 μm) was added. The suspension was vortexed six times, each consisting of 30 s of vortexing followed by at least 30 s of cooling on ice. After the vortexing, 0.75 ml of buffer II was added, and the lysed extract was clarified by centrifugation once at 5,000 × *g* for 5 min and once at 10,000 × *g* for 10 min in a Sorvall centrifuge with an SS34 rotor. An amount of extract corresponding to 16 OD_{260} units was loaded on a 10.5-ml sucrose gradient (7 to 47% sucrose, containing 50 mM Tris-acetate [pH 7.0], 50 mM NH_4Cl, 12 mM $MgCl_2$, 1 mM dithiothreitol, and 0.1% diethylpyrocarbonate). The sucrose gradients were centrifuged at 29,000 rpm for 5.5 h in a Beckman SW41 rotor at 4°C. The gradients were analyzed at 254 nm with a UA-5 UV monitor (ISCO). For analysis at the nonpermissive temperature, strains were shifted to 15°C for 2 h prior to extraction. Dissociation of ribosomes for analysis of steady-state levels of 40S and 60S ribosome subunits was accomplished as described above except that extracts were prepared in buffer II lacking $MgCl_2$ and an amount of extract corresponding to 2.5 OD_{260} units was centrifuged on a 5 to 21% sucrose gradient lacking $MgCl_2$.

Pulse-chase analysis of pre-rRNA processing. The synthesis, processing, and turnover of pre-rRNA were assayed by pulse-chase analysis with [*methyl*-^3H]methionine as described by Deshmukh et al. (14) except that aliquots of yeast cultures were flash frozen in liquid nitrogen prior to RNA extraction. Equal amounts of total RNAs were denatured with glyoxal and separated by agarose gel electrophoresis as described previously (56). Similar procedures were followed for pulse-chase experiments using [^3H]uracil except that strains containing the pRS316 (*CEN3/URA3*) (63) vector were used to allow growth in synthetic complete medium lacking uracil. Densitometric measurement for calculating rRNA levels was performed with an UltroScan XL Laser Densitometer (LKB).

Western immunoblot analysis. To determine the subcellular localization of Dbp3p, we fused a 9-amino-acid hemagglutin (HA) epitope (78) to the C terminus of Dbp3p by a PCR approach using two primers, each containing an engineered *Bam*HI site. The *Bam*HI site (underlined) in primer 3013 (a 27-mer; 5′ cagttGGATCCaaaggggattaaaATG 3′) is located 15 nucleotides (nt) upstream of the initiation codon. Primer 3009 (a 65-mer; 5′ ggGGATCCttatta-[agcatagtc tggaacgtcatatggataatc]-gaaagtaatttttttggttt 3′), which contains the HA epitope (bracketed) followed by two in-frame stop codons, is complementary at its 3′ end to the last 24 nt of the *DBP3* coding sequence. A 1,633-bp DNA fragment amplified from the pCA3001 template DNA by using the Expand High Fidelity polymerase mix (Boehringer Mannheim) was digested with *Bam*HI and cloned into an expression vector. The expression vector, pRS315-pG1, was constructed by transferring the *GPD* promoter-*PGK* terminator cassette from pG1 (58) to pRS315 (64). The *Bam*HI-digested PCR fragment was cloned into the unique *Bam*HI site located between the *GPD* promoter and *PGK* terminator to yield pCA3036. pCA3036 was used to transform a diploid homozygous *dbp3::HIS3* strain, YTC161 (*MAT***a**/α *dbp3::HIS3/dbp3::HIS3 ura3-52/ura3-52 lys2-801/lys2-801 ade2-101/ade2-101 trp1-Δ1/trp1-Δ1 his3-Δ200/his3-Δ200 leu2-Δ1/leu2-Δ1*), to yield YTC207 for subsequent studies.

The *DBP3*-protein A recombinant clone was constructed by inserting, in frame, a 651-bp PCR fragment encoding regions D, A, B, and C of protein A into the *Aat*II site located 37 nt from the stop codon in the *DBP3* open reading frame. The oligonucleotides used to amplify the 651-bp protein A fragment are an upstream (5′ aggtGACGTCcaaaaacttaatgactct 3′) primer and a downstream (5′ ggatGACGTCgttacgttgttcttcagt 3′) primer, each with an engineered *Aat*II site (underlined).

To detect the HA- or protein A-tagged Dbp3p by Western analysis, yeast strains were grown in 100 ml of synthetic dextrose-leucine medium to an OD_{600} of 1. Cells were harvested and broken with glass beads in lysis buffer (50 mM Tris-Cl [pH 7.5], 1 mM dithiothreitol, 1 mM EDTA, 1 mM phenylmethylsulfonyl fluoride). One hundred micrograms of total yeast proteins was separated on an SDS–10% polyacrylamide gel and then transferred to a nitrocellulose membrane by electroblotting. A mouse monoclonal anti-HA antibody (BabCO) was used as the primary antibody at a 1:5,000 dilution, and horseradish peroxidase-conjugated protein G (Bio-Rad) was used as the secondary antibody at a 1:4,000 dilution. Detection of the Dbp3p-HA fusion protein on the membrane was done with the Amersham enhanced chemiluminescence detection system.

Indirect immunofluorescence microscopy. Detection of the cellular Dbp3p-HA protein by indirect immunofluorescence microscopy was done essentially as described previously (32) with minor modifications. Cells were grown to an OD_{600} of 1, collected by filtration, washed extensively in 0.1 M potassium phosphate (pH 6.5), and then fixed in 0.1 M potassium phosphate (pH 6.5) buffer containing 3.7% formaldehyde for 5 min. The formaldehyde-fixed cells were digested with Zymolyase 100T (Sekagaku) for 40 min at 37°C and washed three times in a phosphate-buffered saline solution containing 1 M sorbitol. Cells were treated with −20°C methanol (6 min) and acetone (30 s) and then resuspended in PBL (phosphate-buffered saline, 1 mg of bovine serum albumin per ml, 100 mM lysine), in which the mouse monoclonal anti-HA antibody (BabCO) and rabbit anti-Nop1p polyclonal antiserum (obtained from T. Bergès, European Molecular Biology Laboratory [EMBL]) were added at a 1:100 dilution for staining at room temperature for 3 h. The cells were then washed three times in PBL followed by a 90-min incubation at room temperature with Texas Red-conjugated goat anti-mouse immunoglobulin G and fluorescein isothiocyanate (FITC)-conjugated goat anti-rabbit secondary antibodies (Jackson Laboratories) at a 1:50 dilution. Cells were then washed again in PBL and stained with DAPI (4′,6-diamidino-2-phenylindole) (0.5 μg/ml). Cells were applied to slides with an equal volume of Citifluor (Marivac Ltd.) and visualized by using a Zeiss Axiophot microscope with Normarski optics. Texas Red, FITC, and UV filters were used to detect the fluorescence images.

Construction of the *DBP3*-Δ[KKX]-HA allele. We used a megapriming PCR method (57) to construct the *DBP3*-Δ[KKX]-HA allele. Primer 3010 (a 40-mer; gtacttccacttcccttctcttcaattacctcctcatcta) and primer 3013 (see above) were first used to amplify a 104-bp PCR product from the pCA3001 template. Primer 3010 was designed to anneal to the sense strand of the *DBP3* coding region and remove a 93-bp sequence coding for the following peptide sequence: K, KKS, KKH, KKD, KKD, KKE, KKD, KKH, KKH, KKE, KKG. The PCR product was diluted to 20 μM and used as a megaprimer in a subsequent PCR with primer 3009 (see above) to generate the *DBP3*-Δ[KKX]-HA allele. In the second PCR,

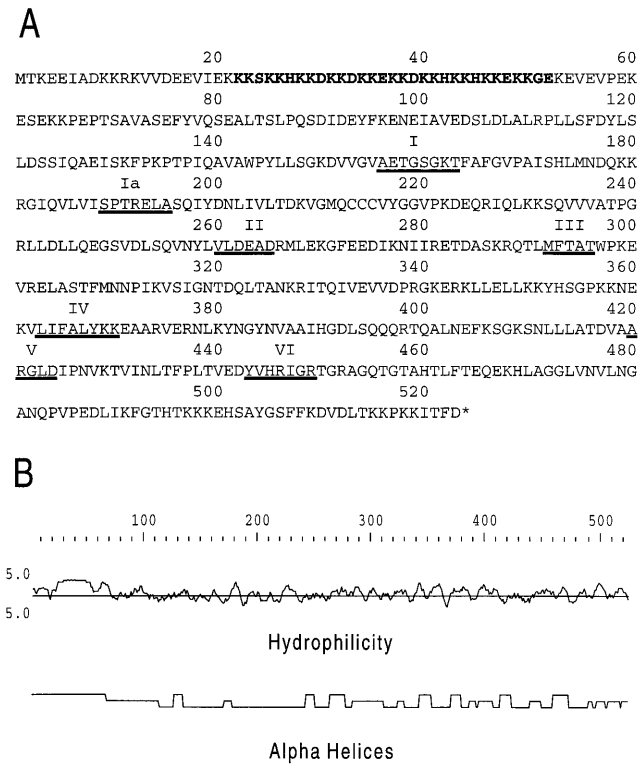

FIG. 2. Predicted amino acid sequence of Dbp3p. (A) Conserved motifs found among the superfamily of putative ATP-dependent RNA helicases are underlined, and the [KKX] repeats are in boldface. The roman numerals denote the nomenclature of the conserved motifs as described by Hodgman (25). (B) Computer prediction of hydrophilicity and alpha-helices of Dbp3p. Computer analysis was done by using the PeptideStructure program in the University of Wisconsin Genetics Computer Group package. Predictions of hydrophilicity and alpha-helices were based on the Kyte-Doolittle (34) and the Chou-Fasman (12) methods.

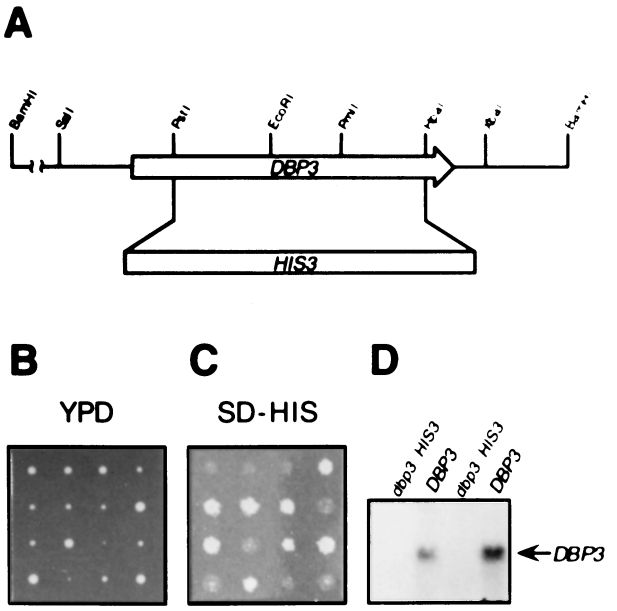

FIG. 3. Genetic disruption of *DBP3*. (A) Restriction map of the *DBP3* locus. The *dbp3::HIS3* allele was constructed by deleting an internal *Pst*I-*Hpa*I *DBP3* fragment and replacing it with the *HIS3* gene. (B) Sporulation and tetrad dissection of strain YTC68 (*dbp3::HIS3*/*DBP3*). Spores were allowed to germinate on a YPD plate at 30°C. A segregation pattern of two small and two large colonies is shown. (C) Cosegregation of the *dbp3::HIS3* allele with the slow-growth phenotype. Cells from the YPD plate in panel B were directly replica plated onto a histidine-dropout synthetic dextrose (SD-HIS) plate and incubated at 30°C overnight. Only the two smaller colonies in a tetrad set are able to grow on the SD-HIS medium, demonstrating 2 His^+:2 His^- segregation and cosegregation of the *HIS3* marker with the slow-growth phenotype. (D) Loss of the *DBP3* transcript cosegregates with the *dbp3::HIS3* allele. Total RNAs from a set of four segregants from panel B were isolated for Northern analysis. A ^{32}P-labeled *Bam*HI fragment was used as a probe to detect the presence of the *DBP3* transcript. The 2.1-kb *DBP3* transcript (9) is present in two His^- segregants but absent in the other two His^+ segregants.

we omitted primer 3009 for the first 10 cycles in order to facilitate extension from the megaprimer. The final 1,540-bp product from the second PCR was digested with *Bam*HI, cloned into the KS(+) vector, and sequenced to verify the precise deletion. The *DBP3*-Δ[KKX]-HA allele was subcloned into the unique *Bam*HI site of the expression vector pRS315-pG1 and transformed into YTC161 for subsequent studies.

RESULTS

***DBP3* encodes a putative RNA helicase with an unusual N terminus.** We have previously identified five novel *DBP* genes in the budding yeast by a PCR approach (10). During initial characterization of their genomic clones, the DNA sequence of the *DBP3* gene became available in GenBank (accession number M80437), enabling us to obtain a complete genomic clone from M. Johnston (Washington University, St. Louis, Mo.). We found that *DBP3* is adjacent to *CTR1* in a head-to-tail fashion on the left arm of chromosome VII. *DBP3* was previously shown to be a single-copy gene (10).

The predicted gene product of *DBP3*, Dbp3p, consists of 523 amino acid residues in which all of the typical DBP conserved motifs can be clearly identified (Fig. 2A). The deduced Dbp3p is highly charged and basic (net overall positive charge, +13; pI = 9.9) and exhibits a hydrophilic N terminus (up to amino acid 65) predicted to adopt an α-helical structure and to position on the protein's surface (Fig. 2B). A rather unusual lysine-lysine-X triplet sequence ([KKX] repeat; X can be either serine, histidine, aspartate, glutamate, or glycine) was found to repeat 10 times between amino acid residues 22 and 51 (Fig. 2A). Similar repeats have been identified in several other proteins (see reference 30 for a summary). These include a glutamic acid-rich protein of unknown function from *Plasmodium falciparum* (72); two microtubule-binding proteins, MAP1A (36) and MAP1B (50); a possible vesicle-associated protein, Torp1, from *Torpedo california* (48); and a yeast protein, Cbf5p, which was isolated as one of the major low-affinity centromere-binding proteins (30). The [KKX] repeats in both MAP1B and Cbf5p have been implicated in their microtubule-binding activities.

Disruption of *DBP3* results in a slow-growth phenotype. To examine whether *DBP3* is an essential gene, we constructed a *dbp3* null allele in vitro by replacing an internal 1.2-kb *DBP3* sequence with a *HIS3* selectable marker (Fig. 3A). This allele was used to transform a wild-type homozygous *his3*$^-$ diploid strain. The resulting His^+ transformants were screened for the correct replacement of one of the two genomic copies of *DBP3* by Southern analysis (data not shown). The verified heterozygous diploids were then subjected to sporulation and tetrad dissection. When allowed to germinate at 30°C, all tetrads gave rise to four viable spores segregating 2 His^+:2 His^- (Fig. 3B and C). Closer inspection of these tetrads revealed that the two His^+ colonies (containing the *dbp3::HIS3* allele) were consistently smaller than the two His^- colonies (containing the wild-type *DBP3* allele). This difference can be further exaggerated by incubating plates at temperatures lower than 30°C. At 16°C,

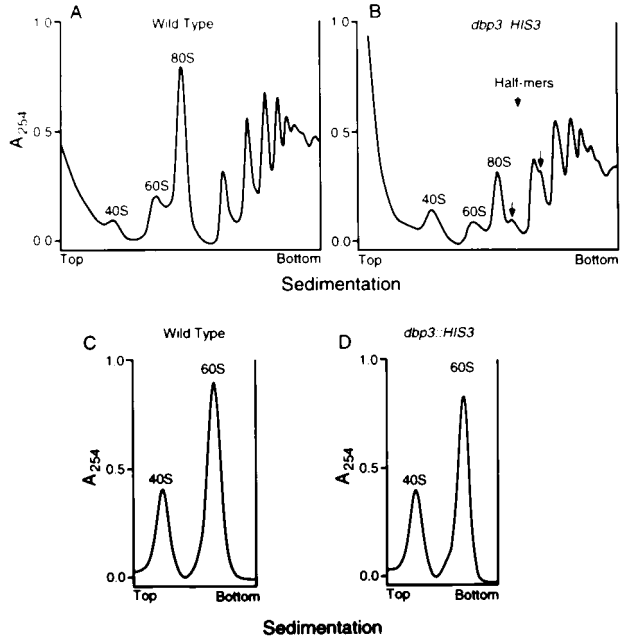

FIG. 4. Genetic disruption of *DBP3* results in a 60S ribosome subunit deficiency. Cell lysates from cultures of the wild-type strain (A) and the *dbp3::HIS3* strain (B) grown at 30°C were prepared for polyribosome profile analysis. Ribosomal subunits and polyribosomes were separated by centrifugation on 7 to 47% sucrose gradients. Peaks representing free 40S and 60S subunits and 80S monosomes are labeled. Locations of half-mer polyribosomes are indicated by arrows. Polyribosome profiles of the *dbp3::HIS3* strain grown at 23 or 16°C are essentially identical to that in panel B. (C and D) Total 40S and 60S subunits in the wild-type (C) and *dbp3::HIS3* (D) strains. Complete dissociation of ribosomes was achieved by preparing extracts in the absence of Mg^{2+} and separating the subunits on 5 to 21% sucrose gradients.

the *dbp3::HIS3* haploid strain appears to have a doubling time twice as long as that of the wild-type haploid. To ascertain whether the slow-growth phenotype is indeed due to the loss of *DBP3* gene expression, the production of the *DBP3* transcript was examined by Northern analysis. Among a set of four segregants derived from a single tetrad, the loss of the 2.1-kb *DBP3* transcript (10) cosegregated with the His^+ as well as the slow-growth phenotype (Fig. 3D).

60S ribosomal subunit deficiency in the *dbp3::HIS3* strain. Although *DBP3* is not essential for cell viability, its requirement for normal cell growth at low temperatures suggests that it is functionally critical in certain biochemical processes that are sensitive to cold temperatures. It has been argued from thermodynamic grounds that mutational defects affecting assembly processes may be intensified at low temperatures (9). Indeed, many cold-sensitive alleles blocking ribosome assembly have been found in bacteria (22, 67). Furthermore, four other DBPs that affect bacterial and yeast ribosome assembly have been identified (49, 51, 55, 71). All of these factors prompted us to inspect ribosome assembly in the *dbp3::HIS3* strain. Sucrose gradient analysis of extracts prepared from *dbp3::HIS3* cells grown at the permissive temperature of 30°C or shifted to 16°C revealed that genetic disruption results in a deficit of 60S ribosomal subunits relative to 40S subunits and also in decreased levels of 80S monosomes and polyribosomes (Fig. 4A and B). The relative reduction of the 60S free subunits was further analyzed by completely dissociating the ribosomes and polyribosomes into 40S and 60S subunits by using extracts prepared in buffer lacking Mg^{2+}. In the *dbp3::HIS3* strain, we observed a 5 to 10% reduction in the overall quantity of 60S subunits relative to that in the wild-type strain (Fig. 4C and D), suggesting a defect in the synthesis or stability of 60S subunits. As a result of the shortage of 60S subunits, half-mer polyribosomes, which contain 43S initiation complexes stalled at the initiator AUG (52), were also detected (Fig. 4B). This defect can be corrected by complementing the *dbp3::HIS3* disruption allele with the wild-type *DBP3* gene carried on a centromere plasmid (data not shown). Finally, we noticed that the relative levels of 60S subunits are indistinguishable in the *dbp3::HIS3* strains grown at either 16, 23, or 30°C.

Delayed formation of 25S rRNA in the *dbp3::HIS3* strain. Since the maturation of rRNAs is closely linked to ribosome subunit formation, we investigated pre-rRNA processing in the *dbp3::HIS3* strain by performing pulse-chase analysis. Cultures were grown to log phase at 25°C, briefly pulse-labeled with either [*methyl*-^{3}H]methionine or [^{3}H]uracil, and then chased with a large excess of cold methionine or uracil, respectively. Aliquots were withdrawn at various times after the chase, total RNA was extracted, and samples were analyzed by agarose gel electrophoresis and fluorography. In the wild-type *DBP3* strain, the 35S pre-rRNA is rapidly processed into 32S pre-rRNA and then into 27S and 20S species, the immediate precursors of the mature 25S and 5.8S rRNAs and the 18S rRNA, respectively (Fig. 5A). However, in the *dbp3::HIS3* strain, we consistently observed a delayed appearance of the 27SA species, which can be easily monitored by comparing the 27SA/27SB ratios at the 1- and 2-min chase points (cf. lanes C1 and C2 in Fig. 5A). This defect can be unambiguously demonstrated by performing the pulse-chase experiment using [^{3}H]uracil (as well as [*methyl*-^{3}H]methionine [data not shown]) as a label at 17°C (Fig. 5B), in which the rate of rRNA processing is reduced, thus avoiding potential errors due to shorter chase time constraints in experiments done at 25°C. Again, the production of 27SA rRNA, and thus 27SB and 25S rRNAs, is clearly delayed in the *dbp3::HIS3* strain (cf. lanes C5 and C15 in Fig. 5B), suggesting that Dbp3p is required for the efficient production of 27SA pre-rRNA. These results predicted that the appearance of 5.8S rRNA, which is generated by processing events occurring after the formation of 27SA pre-rRNA, should also be kinetically delayed in the *dbp3::HIS3* strain (Fig. 1). We analyzed the same RNA samples as used for Fig. 5B by polyacrylamide gel electrophoresis, which allows one to determine potential alterations in the synthesis and processing of smaller RNAs, such as 5.8S and 5S rRNAs and tRNAs. The delayed formation of 5.8S RNA due to upstream cleavage defects is apparent when the C15 and C50 time points for the wild-type and the *dbp3::HIS3* strains were compared (Fig. 5C). Although kinetically delayed, the cleavage pattern leading to the formation of 27SA, 27SB, and 5.8S species in our experiments is in perfect agreement with the established model of the rRNA-processing pathway (Fig. 5A, B, and C). We observed no apparent difference in the ratio of $5.8S_L$ to $5.8S_S$ rRNAs as otherwise found in strains bearing mutations in components of the RNase MRP complex (40, 61, 63), indicating that the alternative 5.8S-processing pathway which yields increased levels of $5.8S_L$ RNA is not preferred in the *dbp3::HIS3* strain. Furthermore, in both [*methyl*-^{3}H]methionine- and [^{3}H]uracil-labeling experiments, we found no evidence of delay in the formation of 18S rRNA through its 20S precursor in the *dbp3::HIS3* strain (Fig. 5A and B), suggesting that the processing of 20S pre-rRNA after cleavage at A_2 site is not impaired in the absence of Dbp3p. Quantitation of the overall RNA methylation efficiency in the pulse-chase experiments by monitoring the radioactivity of the sequentially diluted reaction mixtures revealed that there is no detectable methylation defect in the *dbp3::HIS3* strain (Fig. 5D). Taken together, these

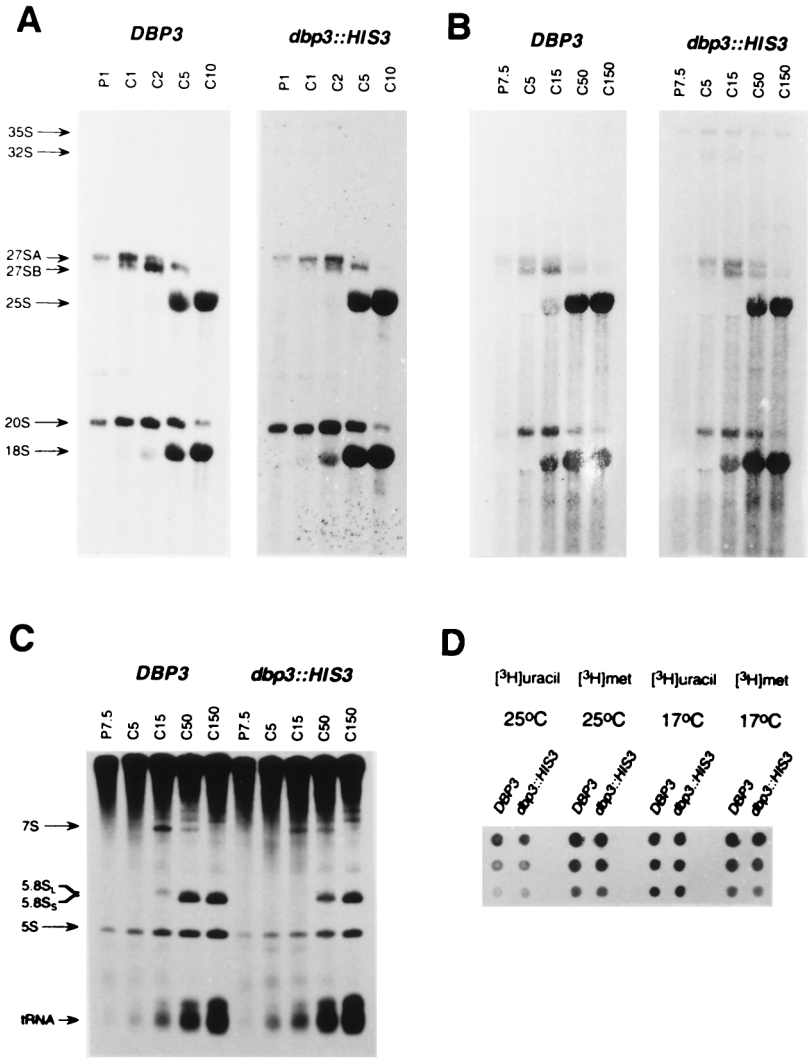

FIG. 5. Delayed 25S rRNA synthesis in the *dbp3::HIS3* strain. Synthesis and processing of pre-rRNA in the wild-type *DBP3* and the *dbp3::HIS3* strains were assayed by a pulse-chase approach. (A) RNA was extracted from cells labeled with [*methyl*-^{3}H]methionine at 25°C for 1 min (lane P1) and chased for 1, 2, 5, and 10 min (lanes C1, C2, C5, and C10) with excess unlabeled methionine. (B) RNA was extracted from cells labeled with [^{3}H]uracil at 17°C for 7.5 min (lane P7.5) and chased for 5, 15, 50, and 150 min (lanes C5, C15, C50, and C150) with excess unlabeled uracil. RNA samples from panels A and B were denatured with glyoxal, run on 1.2% agarose gels, transferred to nylon membranes, sprayed with En^{3}Hance (DuPont), and exposed to film. The positions of mature 25S and 18S rRNAs and their precursors, 35S, 32S, 27SA, 27SB, and 20S, are indicated by arrows. (C) [^{3}H]uracil-labeled RNAs as described for panel B were separated on a polyacrylamide gel which was subsequently soaked in AMPLIFY (Amersham), vacuum dried, and exposed to film. The positions of 7S, 5.8S$_L$, 5.8S$_S$, and 5S rRNAs and tRNAs are indicated by arrows. (D) Serial dilutions of total RNA from [*methyl*-^{3}H]methionine- or [^{3}H]uracil-labeled cultures grown at 25 or 17°C. RNA was vacuum blotted onto nylon membranes, sprayed with En^{3}Hance, and exposed to film.

data suggest that rRNA processing in the *dbp3::HIS3* strain is delayed at steps prior to the formation of the 27SB species.

To further examine the cleavage site(s) affected by the absence of Dbp3p during pre-rRNA processing, we used a series of oligonucleotide probes which hybridize to various regions of the rDNA unit (Fig. 6A) to assess the relative levels of mature and pre-rRNAs in the wild-type and the *dbp3::HIS3* strains by Northern analysis. Probes ITS1-A, ITS1-B, and ITS1-C were used to detect the 20S, 27SA$_2$, and 27SA$_3$ pre-rRNAs (and their precursors), respectively, but not their subsequently processed rRNAs. Probes 18S-A and 25S-A were used to detect mature 18S and 25S rRNAs, respectively; probe 5.8S-A was used to detect pre- and mature rRNAs, namely 27SB, 7S, 5.8S$_L$, and 5.8S$_S$. In addition, probe ETS1-A was employed to assess the relative abundance of the 35S pre-rRNA.

A significant accumulation of the 27SA$_2$ pre-rRNA in the *dbp3::HIS3* strain was detected by probe ITS1-B. 27SA$_2$ pre-rRNA is generated by cleavage at site A$_2$ in ITS1 prior to RNase MRP cleavage at site A$_3$. This suggests that the 25S rRNA-processing delay, as observed in the pulse-chase experiments, is predominantly due to a significant reduction in the rate of the endonucleolytic cleavage at site A$_3$. Probe ITS1-C also detected an accumulation of a 27SA species; however, since this probe will hybridize to both 27SA$_2$ and 27SA$_3$ pre-rRNAs (which cannot be sufficiently resolved in our gel system), this signal is most likely derived from the larger 27SA$_2$ species (see Discussion). We performed primer extension analysis to verify the accumulation of 27SA$_2$ pre-rRNA in the *dbp3::HIS3* strain and to investigate the accuracy of nucleolytic cleavages at sites within ITS1. The signal from the primer extension stop that mapped precisely to site A$_2$ was found to increase dramatically in the *dbp3::HIS3* strain (Fig. 6C),

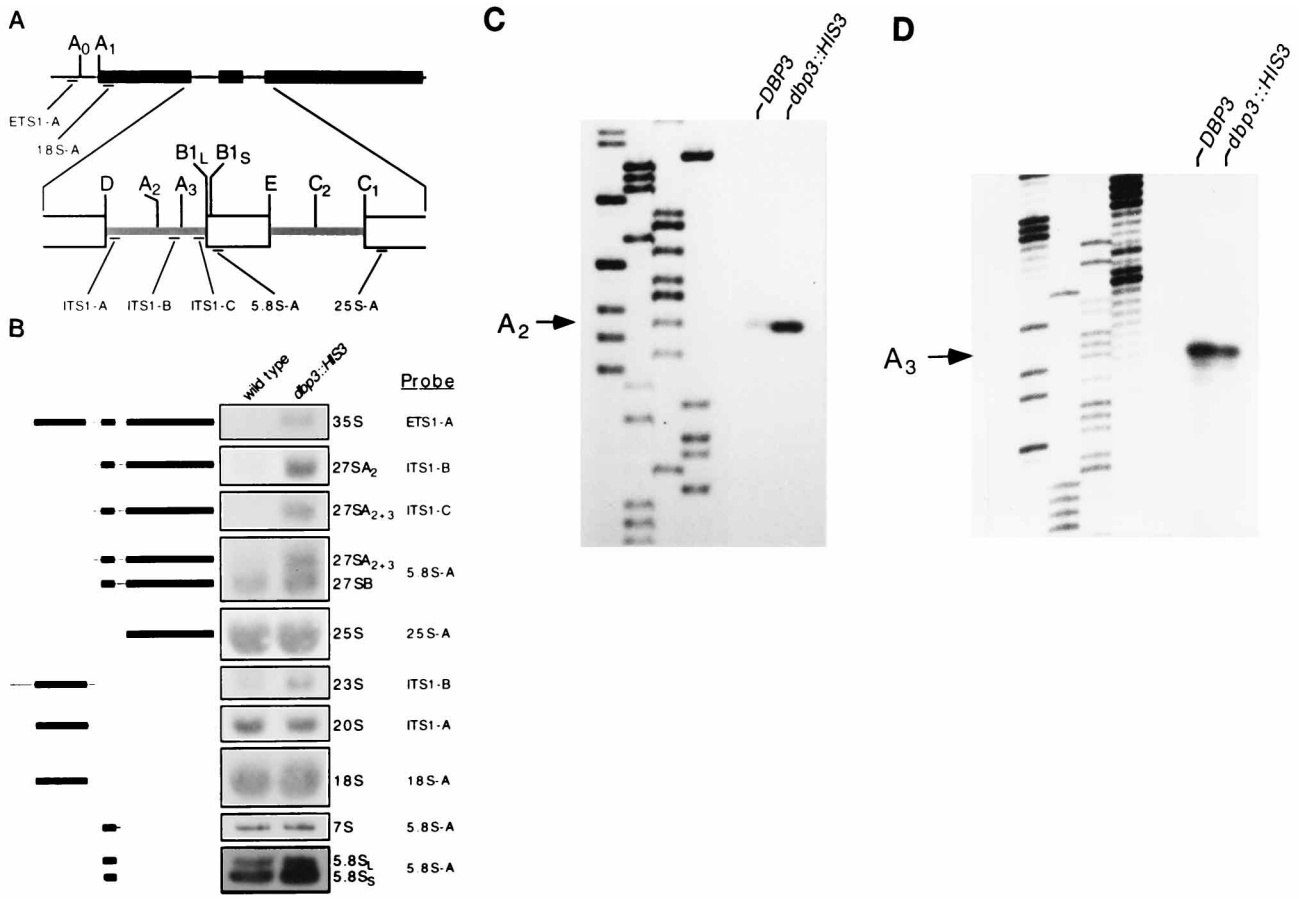

FIG. 6. Analysis of rRNAs from wild-type and *dbp3::HIS3* strains. (A) Structure of the 35S pre-rRNA and positions of oligonucleotide probes. Solid bars represent the mature rRNA sequences, and lines represent the transcribed spacers. The region containing ITS1, 5.8S rRNA, and ITS2 is enlarged for clarity. Regions to which oligonucleotides ETS1-A, 18S-A, ITS1-A, ITS1-B, ITS1-C, 5.8S-A, and 25S-A hybridize are indicated. (B) RNAs were extracted from wild-type and *dbp3::HIS3* strains following growth at 30°C to mid-log phase. The RNAs were denatured with glyoxal, run on 1.2% agarose gels (or polyacrylamide gels for detecting 5.8S and 7S species) and transferred to a nylon membrane for Northern hybridization. For simplicity, only a selected region of each Northern blot is shown. Together these show all the pre-rRNA and rRNA species that we have detected. The positions of various pre-rRNA and rRNA species as detected by various probes are indicated on the right, and their corresponding RNAs are schematically depicted to the left. Solid bars represent the mature rRNA sequences, and thin lines represent the transcribed spacers. (C and D) Primer extension analysis of pre-rRNAs from wild-type and *dbp3::HIS3* strains. Primer extension was performed with oligonucleotide ITS1-B (C) or ITS1-C (D). A dideoxynucleotide sequence generated with the same oligonucleotide was run in parallel. The positions of the A_2 and A_3 cleavage sites are indicated.

whereas the signal from the A_3 stop was decreased as expected in the *dbp3::HIS3* strain (Fig. 6D). In contrast, signals representing stops at sites $B1_L$ and $B1_S$ were indistinguishable between the *dbp3::HIS3* and the wild-type strains (data not shown). Together, these data suggest that in the absence of Dbp3p there is a major processing delay at site A_3 and that later steps leading to the formation of 27SB pre-rRNAs are not significantly hindered. Consistent with this argument, Northern analysis revealed no differences in the $5.8S_L$, $5.8S_S$, and 7S rRNA levels between the wild-type and the *dbp3::HIS3* strains, as determined by probe 5.8S-A (Fig. 6A). This is in contrast to the scenario in which processing events at the 5′ and 3′ ends of the 5.8S rRNA were affected, respectively, by mutations in the RNase MRP complex (13, 41, 61, 63) and *RRP4* (45).

Oligonucleotide probing with ETS1-A, which hybridizes to a region of the pre-rRNA 5′ to the A_0 site, additionally revealed an accumulation of 35S pre-rRNA in the *dbp3::HIS3* strain (Fig. 6B). This accumulation of 35S pre-rRNA has been previously observed in mutants which are defective in cleavages at sites A_2 and A_3 (6, 70) (see Discussion). We also noticed that a 23S-like pre-rRNA shows a mild accumulation in the *dbp3::HIS3* strain as detected by both probes ETS1-A and ITS1-B but not by probe ITS1-C (Fig. 6B). This 23S-like pre-rRNA corresponds most likely to the reported 23S species which accumulates upon deletion of U3 or snR30 RNAs (26, 46). The 23S species, which is generated by an alternate cleavage in the 3′ region of ITS1 upon the impairment of A_2 cleavage, presumably extends from the 5′ end of ETS1 to site A_3 (as discussed in reference 23). Consistent with the pulse-chase data, the processing of the 20S pre-rRNA and the stability of 18S rRNA are not affected in the *dbp3::HIS3* strain, as revealed by probing with the ITS1-A and 18S-A oligonucleotides. Together, these results suggest that the absence of Dbp3p has a major impact on the cleavage efficiency at site A_3 and to a lesser extent at the $A_0/A_1/A_2$ sites and that the kinetic intermediates appearing during the processing events are not degraded. This is in sharp contrast to the situations in *drs1* and *spb4* mutants, where a cessation of 25S rRNA processing results in the eventual degradation of the 25S rRNA precursors (51, 55).

Dbp3p is localized predominantly in the nucleolus. The majority of ribosome assembly and rRNA-processing activities, with the exception of 20S-to-18S rRNA maturation, occur in the nucleolus. On the basis of the biochemical data described

above, it is anticipated that Dbp3p should be present in the nucleolus, if it is directly involved in ribosomal biogenesis. To determine the intracellular location of Dbp3p, we constructed a recombinant Dbp3p clone (Dbp3p-HA) with a 9-amino-acid influenza virus HA epitope (78) fused to its C terminus. We then placed this HA-tagged allele (*DBP3*-HA) under the control of the *GPD* promoter and expressed it in a homozygous *dbp3::HIS3*/*dbp3::HIS3* strain. Western analysis with anti-HA antibodies detected a single 68-kDa protein, in close agreement with the predicted molecular mass of Dbp3p-HA (66 kDa), in extracts prepared from this strain (Fig. 7A). This protein is not detectable in strains expressing only untagged Dbp3p. The facts that expression of the *DBP3*-HA allele can fully restore the 60S ribosomal subunit levels in the *dbp3::HIS3* strain (data not shown) and that the growth of this strain is virtually indistinguishable from that of the wild-type strain suggest that the recombinant protein is fully functional in vivo. The localization of Dbp3p-HA in the homozygous *dbp3::HIS3*/*dbp3::HIS3* strain was then determined by using mouse monoclonal antibodies directed against the HA epitope followed by staining with Texas Red-conjugated goat antimouse antibodies and observing the fixed cells by immunofluorescence microscopy. We observed that the immunofluorescence is restricted only to the nuclear region, with the most intense staining frequently occurring in a crescent-shaped area (Fig. 7C), which presumably corresponds to the yeast nucleolus. The yeast nucleolus has been described as a crescent attached to the nuclear envelope when viewed from certain angles. To confirm nucleolar localization of Dbp3p-HA, we performed double staining by using both mouse anti-HA monoclonal and rabbit anti-Nop1p polyclonal antisera. The anti-Nop1p staining yielded images which can be superimposed with the staining pattern of Dbp3p-HA (Fig. 7D). Interestingly, these crescent-shaped images were consistently located at places which were excluded from the DAPI staining (Fig. 7E). The specificity of this staining was further demonstrated by control experiments using strains which expressed only the untagged Dbp3p. No fluorescence signal could be detected in these strains. To independently confirm the location of Dbp3p, a Dbp3p-protein A recombinant clone was constructed and placed under the control of the native *DBP3* promoter. Expression of this recombinant protein (89 kDa) was demonstrated by Western analysis (Fig. 7A), and the functionality of this protein was confirmed by polyribosome profile analysis as described above (data not shown). Using this strain, we obtained the same staining patterns as for the Dbp3p-HA strain. On the basis of these results, we conclude that Dbp3p is localized predominantly in the nucleolus and is therefore likely to play a direct role in ribosome biogenesis.

Absence of the [KKX] repeats affects Dbp3p's nucleolar localization but not its function in 60S subunit assembly. It has been proposed that if RNA helicases are to function as monomers without the assistance of any accessory proteins, they must contain multiple RNA-binding domains (19). For example, the p68 protein has highly positively charged N- and C-terminal extensions which could potentially interact with substrate RNA. Thus, it is tempting to speculate that the N-terminal [KKX] repeats in Dbp3p may fulfill the same role, which would then predict that the [KKX] repeats are essential for the putative RNA helicase activities of Dbp3p. To investigate this possibility, we constructed a *DBP3*-Δ[KKX]-HA allele, in which the [KKX] repeats (amino acid residues 22 to 51) were deleted from a *DBP3*-HA allele. We then introduced this mutant allele carried on a *CEN* plasmid into a homozygous *dbp3::HIS3*/*dbp3::HIS3* diploid strain. It is predicted that the *DBP3*-Δ[KKX]-HA allele should encode a protein of 56 kDa.

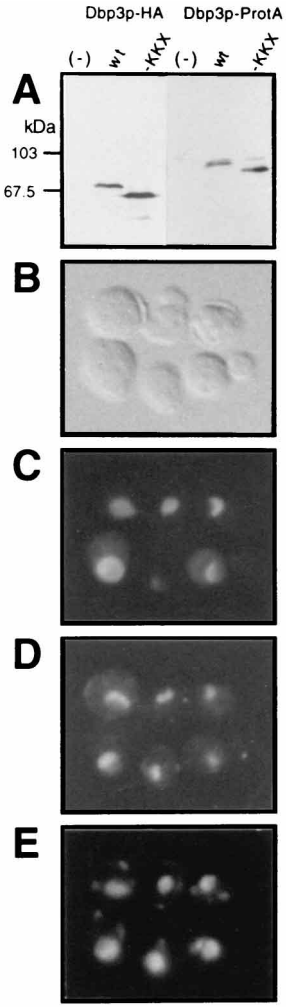

FIG. 7. Dbp3p is localized predominantly in the nucleolus. (A) Expression of the HA-tagged Dbp3p (Dbp3p-HA) and the protein A-fused Dbp3p (Dbp3p-ProtA) in yeast. A 9-amino-acid HA epitope was fused in frame to the C terminus of Dbp3p and a [KKX]-deleted Dbp3p. These two HA-tagged *DBP3* alleles (*DBP3*-HA and *DBP3*-Δ[KKX]-HA) were placed under the control of the *GPD* promoter carried on a *CEN* plasmid and transformed into a homozygous *dbp3::HIS3*/*dbp3::HIS3* diploid strain. Dbp3p-ProtA and its [KKX]-deleted version were constructed in a similar manner except that they were both driven by the native *DBP3* promoter. Protein extracts were isolated from the resulting transformants for identification of the recombinant Dbp3p by Western blotting. The anti-HA monoclonal antibody (BabCO) recognizes a 68-kDa protein in extracts prepared from strains expressing the *DBP3*-HA allele (lane wt, left panel). A 60-kDa protein is detected in extracts made from strains carrying the *DBP3*-Δ[KKX]-HA allele (lane −KKX). (−), extract isolated from a strain harboring only untagged Dbp3p. Purified normal rabbit immunoglobulin G was used to detect protein A-fused Dbp3p (89 kDa; lane wt, right panel) and [KKX]-deleted Dbp3p-ProtA (85 kDa, lane −KKX). (B to E) A *dbp3::HIS3*/*dbp3::HIS3* diploid strain expressing the *DBP3*-HA allele carried on a *CEN* plasmid was harvested, fixed, and permeabilized. For immunostaining we used a mouse monoclonal anti-HA antibody (BabCO) and rabbit anti-Nop1p polyclonal antiserum (obtained from T. Bergès, EMBL) as primary antibodies followed by goat anti-mouse Texas Red-conjugated and goat anti-rabbit FITC-conjugated secondary antibodies (both from Jackson Laboratories). Nuclei were counterstained with 0.5 μg of DAPI per ml to reveal the position of chromosomal DNA, which stains more strongly in the nucleoplasm than in the nucleolus. Cells were visualized with a Zeiss Axiophot microscope with Normarski optics (B); fluorescent images were visualized with Texas Red (C), FITC (D), and DAPI (E) filters.

Western analysis with an anti-HA antibody detected a 60-kDa band (Fig. 7A), in close agreement with the predicted value. The minor bands observed in this blot cannot be reproducibly detected and are likely due to nonspecific interactions. We first

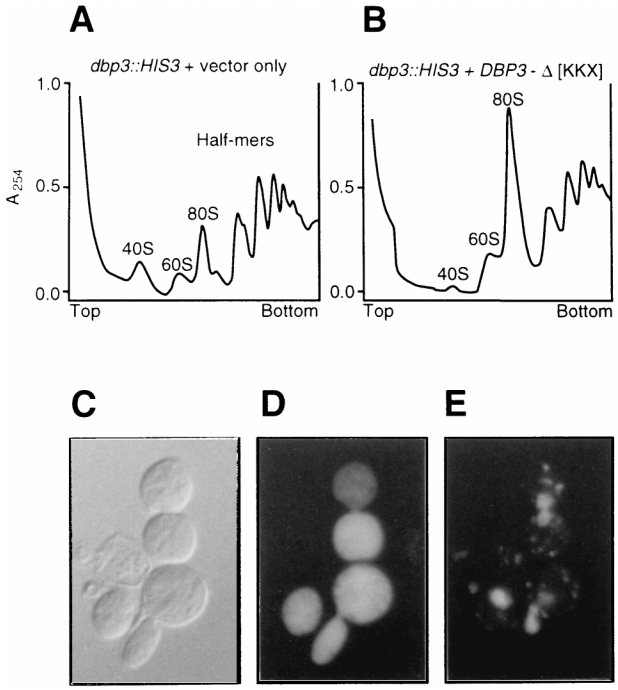

FIG. 8. Deletion of the [KKX] repeats results in Dbp3p mislocalization. (A and B) Complementation of the 60S subunit deficiency in the *dbp3::HIS3* strain by the *DBP3*-Δ[KKX]-HA allele. Cell lysates from a diploid *dbp3::HIS3*/*dbp3::HIS3* strain (A) and from an isogenic strain transformed with the *DBP3*-Δ[KKX]-HA allele carried on a *CEN* plasmid (B) were prepared for polyribosome profile analysis. (C to E) Immunolocalization of Dbp3p-Δ[KKX]-HA. Detection of the deletion mutant Dbp3p by the anti-HA monoclonal antibody was done as described for Fig. 7. (C) Cells viewed by Normarski optics; (D) cells viewed with a Texas Red filter; (E) cells viewed with a DAPI filter.

asked whether the mutant protein without the [KKX] repeats (i.e., Dbp3p-Δ[KKX]-HA) can rescue the 60S subunit assembly defect in the *dbp3::HIS3* background. Polyribosome profile analysis with *dbp3::HIS3* strains carrying the *DBP3*-Δ[KKX]-HA plasmid revealed that the 60S subunit deficiency and the reduction of the polyribosomes were both effectively restored (Fig. 8B), suggesting that the [KKX] repeats are not required for Dbp3p's function in 60S subunit assembly. We then examined the subcellular localization of Dbp3p-Δ[KKX]-HA by indirect immunofluorescence microscopy. Remarkably, in this case, the anti-HA antibody stained the entire cell (Fig. 8D), in sharp contrast to the previous predominantly nucleolar staining of the full-length Dbp3p-HA (Fig. 7C). Interestingly, the staining appears to be distributed evenly over the nucleus and cytoplasm, suggesting that the nuclear import of the mutant protein was not abolished, as would be expected considering that the mutant protein remained functional in ribosome assembly. The same mislocalization pattern was observed when the *DBP3*-Δ[KKX]-HA allele was driven by either the *GPD* promoter or the native *DBP3* promoter, ruling out the possibility that the mislocalization was due to overexpression of the mutant protein. We sought to confirm these results by using a *DBP3*-Δ[KKX]-protein A allele, whose expression is shown in Fig. 7A. We found that the *DBP3*-Δ[KKX]-protein A allele is capable of fully restoring the polyribosomal defects in the *dbp3::HIS3* background, and its gene product is again mislocalized in the same manner as Dbp3p-Δ[KKX]-HA (data not shown). These results thus suggest that the [KKX] repeats are not essential for the putative RNA helicase activity of Dbp3p but are apparently required for sequestering Dbp3p in the nuclear region following protein import (see Discussion).

DISCUSSION

The presence of a large number of RNA helicases in many organisms has raised a number of intriguing questions concerning their cellular functions and their evolutionary relationships. We have chosen to address some of these questions with the budding yeast, where the powerful molecular genetic approach can be used in conjunction with the traditional biochemical approach.

In this work, we showed that Dbp3p is likely to play a direct role in the biogenesis of 60S ribosomal subunits. Most importantly, we demonstrated that upon deletion of the *DBP3* gene, there is a dramatic accumulation of $27SA_2$ pre-rRNA (Figs. 6A and B), a processing intermediate generated after cleavage at site A_2 but prior to cleavage at site A_3 (Fig. 1). This result thus suggests that Dbp3p may facilitate, either directly or indirectly, the efficient cleavage at site A_3, where the RNase MRP complex is currently the sole *trans*-acting factor identified that acts directly upon this site (42). What would be the functional relationship between Dbp3p and RNase MRP? One possibility is that Dbp3p may play an auxiliary role in facilitating rapid cleavage at site A_3 (see below) rather than serving as one of the protein components in the RNase MRP complex. In this scenario, the cleavage at site A_3 would still proceed in the absence of Dbp3p in vivo and in vitro, although predictably at a much slower rate. Several lines of evidence support this argument. Unlike the underproduction of $5.8S_S$ rRNA in *rrp2*/*nme1* (40, 61, 63), *pop1* (41), or *snm1* (62) mutants, which harbor mutations in either the RNA or the protein moiety of RNase MRP, the ratio of the $5.8S_S$ and 5.8_L rRNAs is not altered in the *dbp3::HIS3* strain. In *rrp2*/*nme1*, *pop1*, and *snm1* mutants, the $5.8S_S$ underaccumulation is apparently due to a strong inhibition of cleavage at site A_3, resulting in a predominant cleavage at site $B1_L$ for production of $5.8S_L$ rRNA. Thus, the cleavage at site A_3 in the *dbp3::HIS3* strain may not be affected in the same manner as that influenced by mutations in the RNase MRP components. The facts that the steady-state levels of 25S rRNA in the wild-type and *dbp3::HIS3* strains are virtually indistinguishable (Fig. 6B) and that only a slight reduction of the overall 60S subunit levels is seen in the *dbp3::HIS3* strain (Fig. 4C and D) further underscore the notion that a kinetic delay, rather than an insurmountable block, in pre-rRNA processing occurs in the absence of Dbp3p. Consistent with this, it is noted that *DBP3* is not required for cell viability (Fig. 3), contrasting sharply to the essentiality of *RRP2*/*NME1* and *POP1* genes. Finally, a kinetic role for Dbp3p, rather than a direct involvement in the nuclease attack at site A_3, would be compatible with the observation that the growth rate difference between the wild-type and the *dbp3::HIS3* strains can be exaggerated by lowering the incubation temperature (Fig. 3).

It has been shown that mutations in several snoRNAs (U3, U14, snR10, and snR30) and their protein components (Nop1p, Sof1p, and Gar1p) and in a nucleolar protein, Nsr1p (37), simultaneously affect processing at sites A_0, A_1, and A_2 (reviewed in reference 74), suggesting an association between two distant regions of the pre-rRNA transcript, i.e., the 5′ ETS and ITS1. This led to a proposal that a large processing complex containing multiple snoRNPs is first assembled onto these sites to facilitate a series of rapid and concerted processing reactions (47). Evidence also points to linkage of cleavages at sites A_0/A_1/A_2 to cleavage at site A_3. For example, Allmang et al. (1) have shown that small substitution mutations in the 3′ flanking sequence at site A_2 inhibit processing at site A_3; con-

versely, a small deletion at A_3 delays processing at A_2. In addition, it has been noted that the *rrp2-1* mutation (40, 61), which normally affects cleavage at site A_3, is capable of influencing $A_0/A_1/A_2$ cleavages under more restrictive conditions (cited in reference 2). Depletion of snR30, which results in 18S rRNA maturation defects due to an inhibition of cleavage at site A_2, also yields an accumulation of $27SA_3$ (23). Recently, it was shown that genetic depletion of Rrp5p, a novel protein required for the effective synthesis of 18S and 5.8S rRNAs, can concomitantly impair cleavages at sites A_0, A_1, A_2, and A_3 (75). All of these data support a model in which the processing complexes assembled at sites $A_0/A_1/A_2$ (containing U3, U14, snR10, and snR30 snRNPs) and at site A_3 (containing RNase MRP, Xrn1p [65], and Rat1p [3]) may interact with each other in vivo. The accumulation of 35S pre-rRNA in the *dbp3::HIS3* strain, which suggests that earlier cleavages at sites $A_0/A_1/A_2$ are mildly inhibited, may therefore be explained in light of this model. It is possible that in the absence of Dbp3p, RNase MRP may not gain access to site A_3 in a timely fashion, thereby prohibiting effective communication between A_3 and $A_0/A_1/A_2$ processing complexes and thus delaying early cleavage events in the 35S pre-rRNA. We also observed a mild accumulation of a 23S-like pre-rRNA; the level of this accumulation in the *dbp3::HIS3* strain relative to that in the wild-type strain is approximately 1/10 of that of the $27SA_2$ pre-rRNA as measured by densitometric analysis. We speculate that this 23S-like species may be generated from a subpopulation of the accumulated 35S pre-rRNA which has achieved a conformation permitting cleavage by RNase MRP at or near site A_3 (Fig. 6B). This 23S-like pre-rRNA in the *dbp3::HIS3* strain most likely corresponds to the reported 23S pre-rRNA which spans from the 5′ end of ETS1 to, presumably, site A_3. A 23S precursor has been observed in *nop1* (69), *gar1* (20), snR10 mutant (68), snR30-depleted (46), and U3-depleted (26) strains. However, there remains a possibility that this 23S-like species, as seen in the *dbp3::HIS3* strain, may be generated by RNase MRP cleaving aberrantly at a site(s) between A_3 and the 5′ end of the sequence complementary to probe ITS1-C.

What would be the enzymatic role of Dbp3p, considering its presumed RNA helicase activity? One explanation is that Dbp3p may directly facilitate the attainment of the correct conformation of RNase MRP RNA, which may be required for its optimal activity. However, it is more likely that Dbp3p may play a role in modulating the structure of pre-rRNA either locally or globally for recruiting the RNase MRP complex to site A_3. Site A_3 is located 5 nt downstream of a proposed stable stem-and-loop structure which is adjacent to another upstream, smaller hairpin structure (1, 73). It is conceivable that Dbp3p may function locally to unwind these putative base pairings, thereby permitting an efficient assembly of the RNase MRP complex at site A_3. On the other hand, it is possible that Dbp3p may indirectly affect the cleavage at site A_3 by influencing pre-rRNA folding in a global manner. The discovery of a growing number of snoRNAs exhibiting long stretches of sequence complementarity to conserved sequences in the mature rRNAs has prompted the speculation that these snoRNAs may act as RNA chaperones to catalyze major rearrangements of pre-rRNA at different stages of ribosome biogenesis (reviewed in references 4 and 43). In this scenario, it can be envisioned that Dbp3p may be employed to modulate the structure and function of some of these snoRNAs or to unwind the RNA duplexes formed between snoRNAs and rRNA, thereby indirectly exerting its impact at site A_3.

Alternatively, it is possible that a subpopulation of the 60S subunits in the *dbp3::HIS3* strain is improperly assembled, which could influence the efficiency of pre-rRNA processing and result in the observed slow-growth phenotype. The lack of observable sensitivity of the *dbp3::HIS3* strain to several protein synthesis inhibitors (data not shown) and the lack of any aberrant migration of the 60S subunits in the sucrose gradients (Fig. 4B and D) appear to suggest otherwise. Analysis using a more sensitive method is required to directly address this question in the future.

Two other essential *DBP* genes, *SPB4* (55) and *DRS1* (51), have also been shown to be involved in ribosomal biogenesis. Under nonpermissive conditions, pre-rRNA processing appears to be strongly inhibited at steps prior to the formation of 25S rRNA in both mutants, resulting in a rapid degradation of the pre-rRNAs. This is in contrast to the phenotype we observed in the *dbp3::HIS3* strain, where the production of 25S rRNA is only kinetically delayed, suggesting that the accumulated pre-rRNA, such as $27SA_2$, is not being degraded. Thus, Spb4p and Drs1p are unlikely to be genetically redundant with Dbp3p in ribosomal biogenesis. This is further supported by the fact that overexpression of *SPB4* and *DRS1* as well as several other yeast *DBP* genes, including *PRP28* (66), *DED1* (28), *DBP1* (27), and *DBP5* (previously CA5/6 [10]), on 2μm plasmids cannot replace the function of *DBP3* (data not shown).

Our immunolocalization studies using strains harboring Dbp3p tagged by either an HA or a protein A epitope have demonstrated that Dbp3p is localized predominantly in a nucleolar region superimposable on an area occupied by a well-studied nucleolar protein, Nop1p (Fig. 7). Interestingly, we also detected a less intensive staining signal in the nucleoplasmic region. A similar staining pattern has recently been observed for Rok1p, a novel yeast DBP shown to be involved in 18S rRNA processing (76). Thus, this staining pattern may have a broader implication regarding Dbp3p's cellular functions. It is possible that in addition to its role in ribosomal biogenesis, Dbp3p may have other functions such as the intranuclear transport of factors that affect ribosome assembly and rRNA processing. In this regard, it is noticed that despite its apparent role in pre-rRNA processing (54), Nop3p (also known as Npl3p [8]) has been found to reside predominantly in the nucleoplasm (54) and is capable of shuttling between the nucleus and the cytoplasm (16).

The [KKX] repeats have been found in several proteins other than Dbp3p (30). Among the proteins which contain the [KKX] repeats, the yeast Cbf5p is the best characterized. Cbf5p was identified as a low-affinity centromere-binding protein by chromatography on yeast centromere DNA. However, the physiological relevance of Cbf5p in relation to centromere function is presently unknown. Jiang et al. have reported that a C-terminal deletion that removes all of the $(KKD/E)_n$ repeats plus 20 amino acids downstream is lethal, and cells containing a smaller C-terminal deletion that leaves only three copies of the $(KKD/E)_n$ repeat are delayed in cell cycle progression (30). However, a clean deletion of the $(KKD/E)_n$ region in Cbf5p, leaving the C-terminal region intact, results in no observable phenotype (31). This is consistent with our observation that deletion of the 10 copies of the [KKX] repeats does not diminish Dbp3p's function in 60S subunit assembly (Fig. 8B). Thus, it is unlikely that the [KKX] repeats play an indispensable role in modulating the putative RNA helicase activities of Dbp3p. The facts that Dbp3p is localized predominantly in the nucleolus (Fig. 7) and that deletion of the [KKX] repeats results in a cytoplasmic mislocalization of Dbp3p (Fig. 8C to E) raise an interesting possibility that the [KKX] repeats are playing an important role in nucleolar targeting and/or retention. Support for this hypothesis comes from recent reports that Cbf5p and its mammalian homolog, NAP57, are also

localized in the nucleolus (31, 44). Since the [KKX]-deleted Dbp3p is functional in 60S ribosomal biogenesis (Fig. 8B) and is apparently present in the nucleolar region, and since the [KKX] repeats are not ubiquitous among nucleolar proteins and are not present in NAP57 (44), we believe that it is unlikely to be the sole nucleolar targeting signal. Rather, we favor a scenario in which the [KKX]-deleted Dbp3p can be successfully imported into the nucleolus, where it functions to promote 60S subunit assembly but fails to remain stably associated with the nucleolar compartment. As a result, the [KKX]-deleted Dbp3p may accompany the mature 60S subunit to its final cytoplasmic destination. In this regard, we speculate that the [KKX] repeats could serve as an anchor for interacting with other components, thereby sequestering Dbp3p, and perhaps Cbf5p as well, in the nucleolus.

ACKNOWLEDGMENTS

We thank M. Johnston (Washington University, St. Louis, Mo.) for providing the full-length clone of *DBP3*; A. B. Sachs (University of California, Berkeley) and J. Woolford (Carnegie Mellon University) for providing *SPB4* and *DRS1* clones, respectively; T. Bergès (EMBL) for Nop1p antisera; and J. Aitchison (Rockefeller University) for the protein A clone. We are grateful to J. Woolford for invaluable discussions on polyribosome profile and pre-rRNA-processing analyses, to J. Venema (Vrije Universiteit) for assistance in primer extension analysis, and to K. Jung and B. Oakley (Ohio State University) for instructions on and providing the facility for immunolocalization studies. We acknowledge helpful discussions with M. Rout (Rockefeller University) on immunofluorescence microscopy techniques. We thank W. Jiang, J. Carbon (University of California, Santa Barbara), and J. Venema for communicating their unpublished results and T. McCauley for critical reading of the manuscript.

This work is supported by a setup fund from Ohio State University and an NIH grant (1 R29 GM48752) awarded to T.-H.C.

REFERENCES

1. **Allmang, C., Y. Henry, H. Wood, J. P. Morrissey, E. Petfalski, and D. Tollervey.** 1996. Recognition of cleavage site A_2 in the yeast pre-rRNA. RNA **2:**51–62.
2. **Allmang, C., Y. Henry, J. P. Morrissey, H. Wood, E. Petfalski, and D. Tollervey.** 1996. Processing of the yeast pre-rRNA at sites A_2 and A_3 is linked. RNA **2:**63–73.
3. **Amberg, D. C., A. L. Goldstein, and C. N. Cole.** 1992. Isolation and characterization of *RAT1*: an essential gene of *Saccharomyces cerevisiae* required for the efficient nucleocytoplasmic trafficking of mRNA. Genes Dev. **6:**1173–1189.
4. **Bachellerie, J.-P., B. Michot, M. Nicoloso, A. Balakin, J. Ni, and M. J. Fournier.** 1995. Antisense snoRNAs: a family of nucleolar RNAs with long complementarities to rRNA. Trends Biochem. Sci. **20:**261–264.
5. **Beltrame, M., Y. Henry, and D. Tollervey.** 1994. Mutational analysis of an essential binding site for the U3 snoRNA in the 5′ external transcribed spacer of yeast pre-rRNA. Nucleic Acids Res. **22:**5139–5147.
6. **Bergès, T., E. Petfalski, D. Tollervey, and E. C. Hurt.** 1994. Synthetic lethality with fibrillarin identifies NOP77p, a nucleolar protein required for pre-rRNA processing and modification. EMBO J. **13:**3136–3148.
7. **Blum, S., S. R. Schmid, A. Pause, P. Buser, P. Linder, N. Sonenberg and H. Trachsel.** 1992. ATP hydrolysis by initiation factor 4A is required for translation initiation in *Saccharomyces cerevisiae*. Proc. Natl. Acad. Sci. USA **89:**7664–7668.
8. **Bossie, M. A., C. DeHoratius, G. Barcelo, and P. Silver.** 1992. A mutant nuclear protein with similarity to RNA binding proteins interferes with nuclear import in yeast. Mol. Biol. Cell **3:**875–893.
9. **Cantor, C. R., and P. R. Schimmel.** 1980. Biophysical chemistry, part I. The conformation of biological macromolecules, p. 287–288. W. H. Freeman, San Francisco, Calif.
10. **Chang, T.-H., J. Arenas, and J. Abelson.** 1990. Identification of five putative yeast RNA helicase genes. Proc. Natl. Acad. Sci. USA **87:**1571–1575.
11. **Chang, T.-H.** Unpublished data.
12. **Chou, P. W., and G. D. Fasman.** 1978. Empirical predictions of protein conformation. Annu. Rev. Biochem. **47:**251–276.
13. **Chu, S., R. H. Archer, J. M. Zengel, and L. Lindahl.** 1994. The RNA of RNase MRP is required for normal processing of ribosomal RNA. Proc. Natl. Acad. Sci. USA **91:**659–663.
14. **Deshmukh, M., Y.-F. Tsay, A. G. Paulovich, and J. L. Woolford, Jr.** 1993. Yeast ribosomal protein L1 is required for the stability of newly synthesized 5S rRNA and the assembly of 60S ribosomal subunits. Mol. Cell. Biol. **13:**2835–2845.
15. **Eichler, D. C., and N. Craig.** 1994. Processing of eukaryotic ribosomal RNA. Prog. Nucleic Acid Res. Mol. Biol. **49:**197–239.
16. **Flach, J., M. Bossie, J. Vogel, A. Corbett, T. Jinks, D. A. Willins, and P. A. Silver.** 1994. A yeast RNA-binding protein shuttles between the nucleus and the cytoplasm. Mol. Cell. Biol. **14:**8399–8407.
17. **Fuller-Pace, F. V.** 1994. RNA helicases: modulators of RNA structure. Trends Cell Biol. **4:**271–274.
18. **Fuller-Pace, F. V., S. M. Nicol, A. D. Reid, and D. P. Lane.** 1993. DbpA: a DEAD box protein specifically activated by 23S rRNA. EMBO J. **12:**3619–3626.
19. **Gibson, T. J. and J. D. Thompson.** 1994. Detection of dsRNA-binding domains in RNA helicase A and Drosophila maleless: implications for monomeric RNA helicases. Nucleic Acids Res. **22:**2552–2556.
20. **Girard, J.-P., H. Lehtonen, M. Caizergues-Ferrer, F. Amalric, D. Tollervey, and B. Lapeyre.** 1992. GAR1 is an essential small nucleolar RNP protein required for pre-rRNA processing in yeast. EMBO J. **11:**673–682.
21. **Gururajan, R., L. Mathews, F. J. Longo, and D. L. Weeks.** 1994. An3 mRNA encodes an RNA helicase that colocalizes with nucleoli in *Xenopus* oocytes in a stage-specific manner. Proc. Natl. Acad. Sci. USA **91:**2056–2060.
22. **Guthrie, C., H. Nashimoto, and M. Nomura.** 1969. Structure and function of *E. coli* ribosomes. VII. Cold-sensitive mutants defective in ribosome assembly. Proc. Natl. Acad. Sci. USA **63:**384–391.
23. **Henry, Y., H. Wood, J. P. Morrissey, E. Petfalski, S. Kearsey, and D. Tollervey.** 1994. The 5′ end of yeast 5.8S rRNA is generated by exonucleases from an upstream cleavage site. EMBO J. **13:**2452–2463.
24. **Hirling, H., M. Scheffner, T. Restle, and H. Stahl.** 1989. RNA helicase activity associated with the human p68 protein. Nature **339:**562–564.
25. **Hodgman, T. C.** 1988. A new superfamily of replicative proteins. Nature **333:**22–23.
26. **Hughes, J. M. X., and M. J. Ares.** 1991. Depletion of U3 small nucleolar RNA inhibits cleavage in the 5′ external transcribed spacer of yeast pre-ribosomal RNA and impairs formation of 18S ribosomal RNA. EMBO J. **10:**4231–4239.
27. **Jamieson, D. J., and J. Beggs.** 1991. A suppressor of yeast *spp81/ded1* mutations encodes a very similar putative ATP-dependent RNA helicase. Mol. Microbiol. **5:**805–812.
28. **Jamieson, D. J., B. Rahe, J. Pringle, and J. D. Beggs.** 1991. A suppressor of a yeast splicing mutation (*prp8-1*) encodes a putative ATP-dependent RNA helicase. Nature **349:**715–717.
29. **Jansen, R., D. Tollervey, and E. C. Hurt.** 1993. A U3 snoRNP protein with homology to splicing factor *PRP4* and G beta domains is required for ribosomal RNA processing. EMBO J. **12:**2549–2558.
30. **Jiang, W., K. Middleton, H.-J. Yoon, C. Fouquet, and J. Carbon.** 1993. An essential yeast protein, CBF5p, binds in vitro to centromeres and microtubules. Mol. Cell. Biol. **13:**4884–4893.
31. **Jiang, W., and J. Carbon.** Personal communication.
32. **Kilmartin, J. V., and A. E. M. Adams.** 1984. Structural rearrangements of tubulin and actin during the cell cycle of the yeast *Saccharomyces*. J. Cell Biol. **98:**922–933.
33. **Kiss-László, Z., Y. Henry, J.-P. Bachellerie, M. Caizergues-Ferrer, and T. Kiss.** 1996. Site-specific methylation of preribosomal RNA: a novel function for small nucleolar RNAs. Cell **85:**1077–1088.
34. **Kyte, J., and R. F. Doolittle.** 1982. A simple method for displaying the hydropathic character of a protein. J. Mol. Biol. **157:**105–132.
35. **Lafontaine, D., J. Vandenhaute, and D. Tollervey.** 1995. The yeast 18S rRNA dimethylase Dim1p is required for pre-rRNA processing. Genes Dev. **9:**2470–2481.
36. **Langkopf, A., J. A. Hammarback, R. Muller, R. B. Vallee, and C. C. Garner.** 1992. Microtubule-associated proteins 1A and LC2. Two proteins encoded in one messenger RNA. J. Biol. Chem. **267:**16561–16566.
37. **Lee, W.-C., D. Zabetakis, and T. Mélèse.** 1992. *NSR1* is required for pre-rRNA processing and for the proper maintenance of steady-state levels of ribosomal subunits. Mol. Cell. Biol. **12:**3865–3871.
38. **Li, H. V., J. Zagorski, and M. J. Fournier.** 1990. Depletion of U14 small nuclear RNA (snR128) disrupts production of 18S rRNA in *Saccharomyces cerevisiae*. Mol. Cell. Biol. **10:**1145–1152.
39. **Liang, L., W. Diehl-Jones, and P. Lasko.** 1994. Localization of vasa protein to the *Drosophila* pole plasm is independent of its RNA-binding and helicase activities. Development **120:**1201–1211.
40. **Lindahl, L., R. H. Archer, and J. M. Zengel.** 1992. A new rRNA processing mutant of *Saccharomyces cerevisiae*. Nucleic Acids Res. **20:**295–301.
41. **Lygerou, Z., P. Mitchell, E. Petfalski, B. Séraphin, and D. Tollervey.** 1994. The *POP1* gene encodes a protein component common to the RNase MRP and RNase P ribonucleoproteins. Genes Dev. **8:**1423–1433.
42. **Lygerou, Z., C. Allmang, D. Tollervey, and B. Séraphin.** 1996. Accurate processing of a eukaryotic precursor ribosomal RNA by ribonuclease MRP in vitro. Science **272:**268–270.
43. **Maxwell, E. S., and M. J. Fournier.** 1995. The small nucleolar RNAs. Annu. Rev. Biochem. **35:**897–934.
44. **Meier, U. T., and G. Blobel.** 1994. NAP57, a mammalian nucleolar protein

with a putative homolog in yeast and bacteria. J. Cell Biol. **127:**1505–1514.
45. **Mitchell, P., E. Petfalski, and D. Tollervey.** 1996. The 3′ end of yeast 5.8S rRNA is generated by an exonuclease processing mechanism. Genes Dev. **10:**502–513.
46. **Morrissey, J. P., and D. Tollervey.** 1993. Yeast snR30 is a small nucleolar RNA required for 18S rRNA synthesis. Mol. Cell. Biol. **13:**2469–2477.
47. **Morrissey, J. P., and D. Tollervey.** 1995. Birth of the snoRNPs: the evolution of RNase MRP and the eukaryotic pre-rRNA-processing system. Trends Biochem. Sci. **20:**78–82.
48. **Ngsee, J. K., and R. H. Scheller.** 1989. Isolation and characterization of two homologous cDNA clones from *Torpedo* electromotor neurons. DNA **8:**555–561.
49. **Nishi, K., F. Morel-Deville, J. W. B. Hershey, T. Leighton, and J. Schnier.** 1988. An eIF-4A-like protein is a suppressor of an *Escherichia coli* mutant defective in 50S ribosomal subunit assembly. Nature **336:**496–498.
50. **Noble, M., S. A. Lewis, and N. J. Cowan.** 1989. The microtubule binding domain of microtubule-associated protein MAP 1B contains a repeated sequence motif unrelated to that of MAP2 and tau. J. Cell Biol. **109:**3367–3376.
51. **Ripmaster, T. L., G. P. Vaughn, and J. L. Woolford, Jr.** 1992. A putative ATP-dependent RNA helicase involved in *Saccharomyces cerevisiae* ribosome assembly. Proc. Natl. Acad. Sci. USA **89:**11131–11135.
52. **Rotenberg, M. O., M. Moritz, and J. L. Woolford, Jr.** 1988. Depletion of *Saccharomyces cerevisiae* ribosomal protein L16 causes a decrease in 60S ribosomal subunits and formation of half-mer polyribosomes. Genes Dev. **2:**160–172.
53. **Rozen, F., I. Edery, K. Meerovitch, T. E. Dever, W. C. Merrick, and N. Sonenberg.** 1990. Bidirectional RNA helicase activity of eucaryotic translation initiation factors 4A and 4F. Mol. Cell. Biol. **10:**1134–1144.
54. **Russell, I. D., and D. Tollervey.** 1992. NOP3 is an essential yeast protein which is required for pre-rRNA processing. J. Cell Biol. **119:**737–747.
55. **Sachs, A. B., and R. W. Davis.** 1990. Translation initiation and ribosomal biogenesis: involvement of a putative rRNA helicase and *RPL46*. Science **247:**1077–1079.
56. **Sambrook, J., E. F. Fritsch, and T. Maniatis.** 1989. Molecular cloning: a laboratory manual, 2nd ed. Cold Spring Harbor Laboratory Press, Cold Spring Harbor, N.Y.
57. **Sarkar, G., and S. S. Sommer.** 1990. The "megaprimer" method of site-directed mutagenesis. BioTechniques **8:**404–407.
58. **Schena, M., D. Picard, and K. R. Yamamoto.** 1991. Vectors for constitutive and inducible gene expression in yeast. Methods Enzymol. **194:**389–398.
59. **Schimmang, T., D. Tollervey, H. Kern, R. Frank, and E. C. Hurt.** 1989. A yeast nucleolar protein related to mammalian fibrillarin is associated with small nucleolar RNA and is essential for viability. EMBO J. **8:**4015–4924.
60. **Schmid, S. R., and P. Linder.** 1992. D-E-A-D protein family of putative RNA helicases. Mol. Microbiol. **6:**283–292.
61. **Schmitt, M. E., and D. A. Clayton.** 1993. Nuclear RNase MRP is required for correct processing of pre-5.8S rRNA in *Saccharomyces cerevisiae*. Mol. Cell. Biol. **13:**7935–7941.
62. **Schmitt, M. E., and D. A. Clayton.** 1994. Characterization of a unique protein component of yeast RNase MRP: an RNA-binding protein with a zinc-cluster domain. Genes Dev. **8:**2617–2628.
63. **Shuai, K., and J. W. Warner.** 1991. A temperature sensitive mutant of *Saccharomyces cerevisiae* defective in pre-rRNA processing. Nucleic Acids Res. **19:**5059–5064.
64. **Sikorski, R. S., and P. Hieter.** 1989. A system of shuttle vectors and yeast host strains designed for efficient manipulation of DNA in *Saccharomyces cerevisiae*. Genetics **122:**19–27.
65. **Stevens, A., C. L. Hsu, K. R. Isham, and F. W. Larimer.** 1991. Fragments of the internal transcribed spacer 1 of pre-rRNA accumulate in *Saccharomyces cerevisiae* lacking 5′→3′ exoribonuclease 1. J. Bacteriol. **173:**7024–7028.
66. **Strauss, E. J., and C. Guthrie.** 1991. A cold sensitive mRNA splicing mutant is a member of the RNA helicase gene family. Genes Dev. **5:**629–641.
67. **Tai, P. C., D. P. Kessler, and J. Ingraham.** 1969. Cold-sensitive mutations in *Salmonella typhimurium* which affect ribosome synthesis. J. Bacteriol. **97:**1298–1304.
68. **Tollervey, D.** 1987. A yeast small nuclear RNA is required for normal processing of pre-ribosomal RNA. EMBO J. **6:**4169–4175.
69. **Tollervey, D., H. Lehtonen, M. Carmo-Fonseca, and E. C. Hurt.** 1991. The small nucleolar RNP protein NOP1 (fibrillarin) is required for pre-rRNA processing in yeast. EMBO J. **10:**573–583.
70. **Tollervey, D., H. Lehtonen, R. Jansen, H. Kern, and E. C. Hurt.** 1993. Temperature-sensitive mutations demonstrate roles for yeast fibrillarin in pre-rRNA processing, pre-rRNA methylation, and ribosome assembly. Cell **72:**443–457.
71. **Toone, W. M., K. E. Rudd, and J. D. Friesen.** 1991. *deaD*, a new *Escherichia coli* gene encoding a presumed ATP-dependent RNA helicase, can suppress a mutation in *rpsB*, the gene encoding ribosomal protein S2. J. Bacteriol. **173:**3291–3302.
72. **Triglia, T., H.-D. Stahl, P. E. Crewther, A. Silva, R. F. Anders, and D. J. Kemp.** 1988. Structure of a *Plasmodium falciparum* gene that encodes a glutamic acid-rich protein (GARP). Mol. Biochem. Parasitol. **31:**199–202.
73. **Van Nues, R. W., J. M. J. Rientjes, C. A. F. M. Van der Sande, S. F. Zerp, C. Sluiter, J. Venema, R. J. Planta, and H. A. Raué.** 1994. Separate structural elements within internal transcribed spacer 1 of *Saccharomyces cerevisiae* precursor ribosomal RNA direct the formation of 17S and 26S rRNA. Nucleic Acids Res. **22:**912–929.
74. **Venema, J., and D. Tollervey.** 1996. Processing of pre-ribosomal RNA in *Saccharomyces cerevisiae*. Yeast **11:**1629–1650.
75. **Venema, J., and D. Tollervey.** 1996. *RRP5* is required for formation of both 18S and 5.8S rRNA in yeast. EMBO J. **15:**5701–5714.
76. **Venema, J., and D. Tollervey.** Personal communication.
77. **Vijayraghavan, U., M. Company, and J. Abelson.** 1989. Isolation and characterization of pre-mRNA splicing mutants of *Saccharomyces cerevisiae*. Genes Dev. **3:**1206–1216.
78. **Wilson, I. A., H. L. Niman, R. A. Houghten, A. R. Cherenson, M. L. Connolly, and R. A. Lerner.** 1984. The structure of an antigenic determinant in a protein. Cell **37:**767–778.
79. **Woolford, J. L., Jr., and J. R. Warner.** 1991. The ribosome and its synthesis, p. 587–626. *In* J. R. Broach, J. R. Pringle, and E. W. Jones (ed.), The molecular biology of the yeast *Saccharomyces*: genome dynamics, protein synthesis, and energetics. Cold Spring Harbor Laboratory Press, Cold Spring Harbor, N.Y.